Original Article

Int Neurourol J 2022;26(3):210-218
https://doi.org/10.5213/inj.2244202.101
pISSN 2093-4777 · eISSN 2093-6931

INTERNATIONAL NEUROUROLOGY JOURNAL
INJ
OPEN ACCESS

A Study on the Optimal Artificial Intelligence Model for Determination of Urolithiasis

Sung-Jong Eun[1], Myoung Suk Yun[1], Taeg-Keun Whangbo[2], Khae-Hawn Kim[3]

[1]Digital Health Industry Team, National IT Industry Promotion Agency, Jincheon, Korea
[2]Department of Computer Science, Gachon University, Seongnam, Korea
[3]Department of Urology, Chungnam National University Sejong Hospital, Chungnam National University College of Medicine, Sejong, Korea

Purpose: This paper aims to develop a clinical decision support system (CDSS) that can help detect the stone that is most important to the diagnosis of urolithiasis. Among them, especially for the development of artificial intelligence (AI) models that support a final judgment in CDSS, we would like to study the optimal AI model by comparing and evaluating them.
Methods: This paper proposes the optimal ureter stone detection model using various AI technologies. The use of AI technology compares and evaluates methods such as machine learning (support vector machine), deep learning (ResNet-50, Fast R-CNN), and image processing (watershed) to find a more effective method for detecting ureter stones.
Results: The final value of sensitivity, which is calculated using true positive (TP) and false negative and is a measure of the probability of TP results, showed high recognition accuracy, with an average value of 0.93 for ResNet-50. This finding confirmed that accurate guidance to the stones area was possible when the developed platform was used to support actual surgery.
Conclusions: The general situation in the most effective way to the detection stone can be found. But a variety of variables may be slightly different the difference through the term could tell. Future works, on urological diseases, are diverse and the research will be expanded by customizing AI models specialized for those diseases.

Keywords: Urolithiasis; Ureter stones; ResNet-50; Fast R-CNN; Surgical support technology

- **Funding/Grant Support:** This study was supported by Chungnam National University Sejong Hospital Research Fund, 2022.
- **Research Ethics:** This research was approved by the Institutional Review Board of Chungnam National University Hospital (approval number: CNUIRB2022-068).
- **Conflict of Interest:** KHK, the corresponding author of this article, is the editor-in-chief of INJ. However, KHK played no role whatsoever in the editorial evaluation of this article or the decision to publish it. No potential conflict of interest relevant to this article was reported.

- ***HIGHLIGHTS***
  - This paper propose an optimal ureter stone detection model using various artificial intelligence (AI) technologies. We would like to study the optimal AI model by comparing and evaluating them.

Corresponding author: Khae-Hawn Kim
https://orcid.org/0000-0002-7045-8004
Department of Urology, Chungnam National University Sejong Hospital, Chungnam National University College of Medicine, 20 Bodeum 7-ro, Sejong 30099, Korea
Email: kimcho99@cnuh.co.kr
Co-corresponding author: Taeg-Keun Whangbo
https://orcid.org/0000-0003-1409-0580
Department of Computer Science, Gachon University, 1342 Seongnam-daero, Sujeong-gu, Seongnam 13120, Korea
Email: tkwhangbo@gachon.ac.kr
Submitted: September 2, 2022 / **Accepted after revision:** September 22, 2022

INTRODUCTION

Urolithiasis [1-8] is a disease in which substances in urine make decisions and harden like stones in the kidneys and move along the urinary tract. Therefore, urolithiasis is closely related to water intake. A decrease in water intake increases the probability of urinary stones occurring by increasing the amount of time they stay in the urine. Also, in the case of children whose parents have urinary stones, the incidence rate increases due to genetic effects. In general, men are known to have twice the risk of developing them than women, and by age, the incidence rate is relatively high in young people in their 20s and 40s.

Urolithiasis is caused by reduced water intake resulting in longer urinary retention of urinary stones. The incidence of men is higher than that of women, and it occurs more often in young age groups. Temperature and season also play an important role in the occurrence of urinary stones. If you sweat a lot in summer, urine can be concentrated and ureter stones can occur easily. Stone from the kidney moves along the transition part of the renal ureter, ureter, bladder, and urethra, interfering with urine flow and causing extreme pain. In the process, urinary tract infections, hydropathy, as well as kidney failure can be impaired. If ureteral stones are not resolved, partial or complete obstruction of the urethra may persist, leading to reception and kidney failure. It may be accompanied by local irritation and urinary tract infections caused by stones.

Urolithiasis is finally confirmed through a patient's symptoms, physical examination, urine test, and radiation test. The diagnosis is diagnosed by the patient's clinical symptoms, physical examination, and urinary examination, and is finally confirmed through radiation examination. Although simple urinary tract imaging can confirm stone, simple radiation cannot diagnose invisible stones. Also, ureter stones may be obscured by the pelvic bone or may be obscured by feces or other organs, making it difficult to be difficult to distinguish. This allows ureteral stones to be checked by urography or computed tomography (CT). In many cases, it may be difficult to confirm the presence of stone, which is an important part of the clinician's diagnosis.

Therefore, this paper aims to develop a clinical decision support system (CDSS) that can help detect the stone that is most important to the diagnosis of urolithiasis. Among them, especially for the development of artificial intelligence (AI) models that support a final judgment in CDSS, we would like to study the optimal AI model by comparing and evaluating them.

The application of AI has been initiated in various medical fields. There is no exception to the urological system, and AI research is actively being conducted in the whole cycle of analysis, diagnosis, treatment, and management of urological diseases. Most of them are being studied as an auxiliary means of patient care, and the proportion of model research, which is a key technology, is high. In the case of overseas research trends, it can be seen as an AI imaging solution field, and not only small manufacturers but also large medical device companies are investing in innovative AI medical imaging solution R&D projects. The status of medical devices approved by the U.S. Food and Drug Administration accounts for more than 90% of imaging medical devices, and is licensed to assist doctors in diagnosing.

In the case of AI technology in the urolithiasis field, there are not many related intellectual rights, so if R&D and commercialization are successful, market preoccupation effects can be expected. Various studies of AI models specialized in urolithiasis disease are needed, and it is important to find the optimal form suitable for clinical sites.

Based on these parts, this paper conducts research on the optimal AI model for finding stone in urolithiasis disease. The performance method is to find the most suitable method for diagnostic assistance by applying an AI model that finds the presence of stone and location from various angles.

MATERIALS AND METHODS

This paper proposes the optimal ureter stone detection model using various AI technologies. The use of AI technology compares and evaluates methods such as machine learning, deep learning, and image processing to find a more effective method for detecting ureter stones. The machine learning method is a representative segmentation method, support vector machine (SVM), and deep learning is a representative convolutional neural networks (CNN) method, and ResNet-50 [9-13] and Fast R-CNN, and image processing is an efficient watershed method for circular objects considering the shape information of stones. Comparative evaluation of this method is performed by applying it to abdominal CT images of urolithiasis patients. This will be explained in the next chapter. Fig. 1 presents a conceptual diagram of the proposed method.

CNN-Based Technology to Object Detection

Numerous studies in the medical field have applied image recognition, voice classification, recognition, and object detection

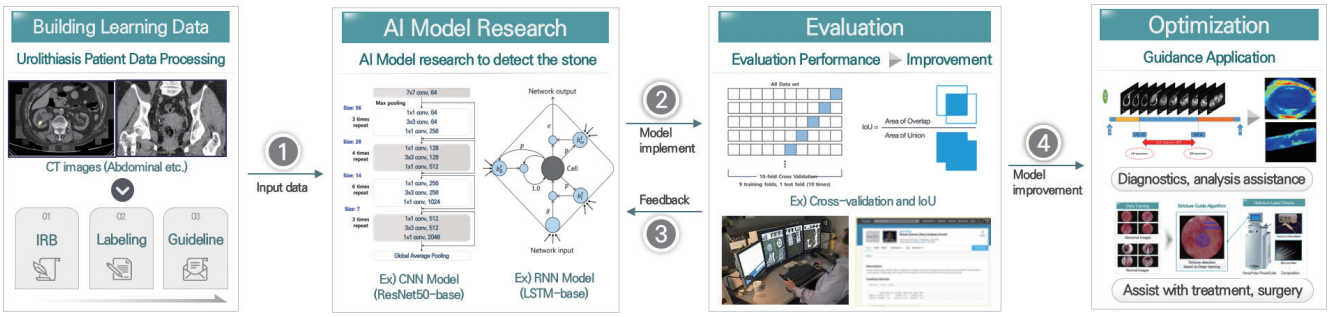

Fig. 1. The conceptual diagram of the proposed method. IRB, Institutional Review Board; CNN, convolutional neural networks; LSTM, long short-term memory model.

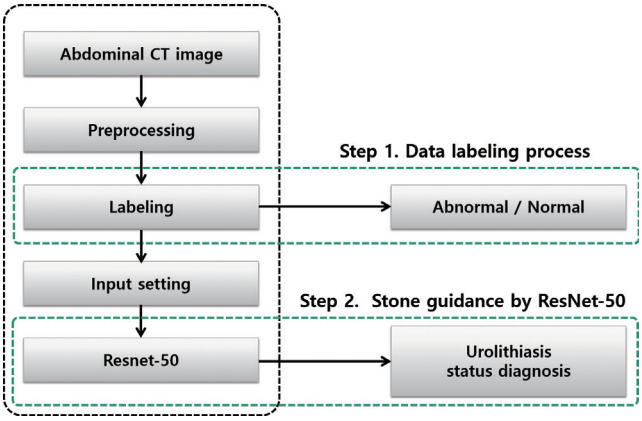

Fig. 2. The flow of urolithiasis status guidance algorithm.

through deep learning, which has demonstrated good performance in the machine learning field due to advances in high-performance hardware and big data. Among them, CNN [14], which are widely used in image recognition, are deep learning models developed to overcome overfitting, local optimal convergence, and gradient extinction by modifying the structure of the existing artificial neural networks. Lecun [15] constructed a model that took 32×32 black-and-white images with handwritten text as input to recognize cursive writing and generated 10 numbers as outputs, but this model did not receive much attention due to long-term learning problems. The speed of CNN has improved significantly due to high-performance hardware and big data development. It is easy to collect the data necessary for supervised and unsupervised learning, with representative picture-sharing services including ImageNet [16], Flickr [17], and the INRIA Person dataset [18]. Introducing the algorithm presented by Zeller and Fergus [19] for the existing overfitting problem has solved many problems and yielded excellent performance in object classification and detection. CNN is better than conventional object detection and learning methods at automatically detecting shapes from input images, and they have the advantage of extracting and learning shapes from one structure.

ResNet-50

We provide guidance for identifying urolithiasis by applying ResNet-50. The process of the algorithm is shown in Fig. 2. Compared to conventional object segmentation and identification methods, a system using a deep convolutional neural network (DCNN) called AlexNet [20] showed remarkable recognition performance, prompting further research on deep neural networks. The reason for this high level of performance is that increasing the depth and width of the CNN is expected to improve the recognition performance, so the system can iterate the basic structure of the CNN repeatedly to extract low medium and high-level functions. However, as the depth and width of the neural network increase, the problem of increasing parameters and computational quantities for learning must be solved. To reduce the number of parameters to be learned, GoogleNet [21] introduced a startup module that sparsely connects large neural networks to make neural networks deeper. In the development of ResNet, it is found that increasing the model depth of DCNN increases errors in the learning process, leading researchers to introduce shortcut connections to minimize these learning errors.

The DCNN model has the advantage of being able to solve the vanishing gradient problem leading to backpropagation in the learning process because it does not significantly change the structure of existing networks, so the number of parameters to learn does not increase even if the depth of DCNN increases. For this reason, instead of optimizing weights across the entire

neural network, partial learning is performed on each residual block consisting of 2 to 3 layers [22]. The ResNet-50 model is a deep learning method with 50 convolutional layers, which aims to enhance stenosis detection by learning with ImageNet weights obtained using data from more than 3 million real-world images. The ResNet-50 model resizes images to 512×512 dimensions, processes images in real-time, performs image preprocessing to reconstruct pixel ranges (–128 to +128), and transforms images (zoom, shrink, rotate, and move) on learning to adapt to various changes.

In this paper, the learning parameters were as follows: epoch number, 100; batch size, 12; learning rate: 0.001–0.00001; anchor size, 32, 64, 128, 256, or 512; anchor ratios, 0.5, 1, or 2; and anchor scales, 1, $2^{1/3}$, or $2^{2/3}$). Fig. 3 shows the structure of ResNet-50 that was applied for actual detection. The structure of ResNet-50 representing this can be found in below Fig. 3.

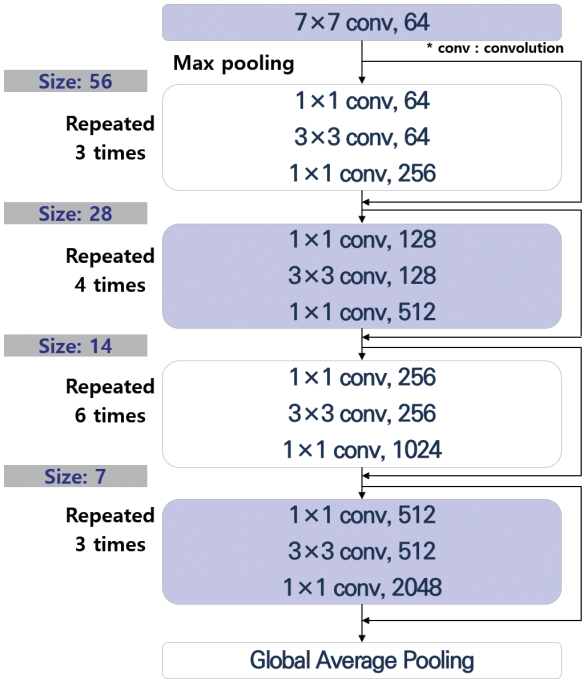

Fig. 3. The structure of ResNet-50.

Fast R-CNN

R-CNN, regions with CNN features performs affine image warping in each study area as one of the area-based deep learning technique and then use selective search to create region proposal. A selective search algorithm [23] based on the bottom-up approach amalgamates or removes areas by measuring similarity over each area. R-CNN extracts 227×227 feature vectors through CNN structure from the learning area which performed a selective search algorithm and then classifies it by using linear independent SVM. R-CNN has a disadvantage in that has complex structure and creates 2,000 candidate area to verify each area leading to increased amount of calculation as it provides CNN structures as many as learning areas and problems of image deformation and loss because it affine image warps and crops each learning area in input image. To overcome these shortcomings, Fast R-CNN [24] is proposed.

Fast R-CNN is one of the domain-based deep learnings that generates feature maps using a convolution network, excluding a fully connected layer, of input images and learning regions (RoI). We perform an RoI Pooling layer that extracts fixed-length feature vectors from feature maps so that various learning areas can enter the fully connected layer. After extracting the feature through the RoI Pooling layer, it is learned through the complete connection layer. After learning, classifier and bounding box regression, which are object detection parts, are classified using softmax and cross entropy, and the detection area is predicted. In R-CNN, problems such as problems where CNN features cannot be updated in response to linearly independent SVM and object region coordinates, and problems with complex learning structures are solved using multi-task loss in Fast R-CNN and end-to-end learning structures. This method is applied to detect stones of urolithiasis patients.

SVM-Based Technology to Object Detection

In this paper, radial basis function (RBF)-based SVM [25] is applied to detect a stone site. Support vectors are data points located at the boundary between 2 classes. There is a lot of data, but support vectors among them influence the creation of decision boundaries. However, most data are not ideally separated. In many cases, outliers are observed. In this case, it is impossible to isolate the data linearly and completely. To solve this problem, a strategy has been created to allow some errors. The parameter associated with this is cost. Cost determines how many data samples are allowed to be placed in different classes. The smaller, the more allowed, and the larger, the less allowed. In other words, setting a low-cost value greatly captures the possibility of anomalies and finds general decision boundaries, while setting a high setting makes the possibility of an ideal smaller, making it more careful. Also, kernel technology is to think of the given data as a high-level characteristic space. Once it is thought of in a high-dimensional space, it can be classified into linear or nonlinear shapes that were not seen in the origi-

nal dimension. For the RBF kernel, the parameter gamma must be adjusted by the user. Gamma is associated with the standard deviation of the Gaussian function, and the larger, the smaller the standard deviation. In other words, the larger the gamma, the shorter the distance a data pointer exerts influence, while the lower the gamma, the larger the gamma. Through this, it is simultaneously determined by combining the boundary connection characteristics of the stone and the pixel intensity characteristics.

Image Processing to Object Detection

In order to detect the circular shape of stones, the watershed [26] was applied as an image processing method. The principle of the watershed algorithm is that when the slope is obtained from the original image, the gray level has a high value and a low value, which is a method of analyzing the image by viewing the slope in a topographical sense. In addition, the watershed algorithm assumes that there is a hole at the minimum value of the slope image, and water starts to rise little by little through the hole and starts to merge into another pool, making it impossible to merge. A line composed of these dams is expressed as a watershed line, and an image included in the watershed line is divided.

The watershed algorithm has a problem of overdivision because it expands the area based on the regional minimum. Marker control watershed are a way to determine external and internal markers as a way to control this overdivision, and to correct the calculated slope again to solve the problem of overdivision. The selection of markers varies from a simple method to a range of sizes, shapes, location relative distances, and textures. What is important here is that the use of markers introduces prior knowledge related to the segmentation problem.

Since finding the presence of stones should be preceded, this paper determines the presence or stone of an object before separation of adjacent area objects. In order to find the stone, a marker based on shape and pixel value was applied to the corresponding watershed algorithm.

The Construction of Evaluation Data

Evaluation data of 150 CT images were constructed to evaluate the performance of various analysis methods. Among them, it was composed of patients and normal people at a ratio of 50:50. The construction of learning data for urolithiasis patients is largely carried out through 4-step work. It is constructed through the process of generating, processing, loading, and security of data. Data generation is collected for in-hospital research purposes through hospital Institutional Review Board deliberation. The processing is anonymized for the wall of erosion included in the data. And it is processed into learning data through data labeling. Data loading refers to the loading of deidentified learning data on a data server in a hospital. Since then, security is to design policies such a3s access management and permission management of data and to reflect them in the data server to support security in research.

Comparative Evaluation and Statistical Analysis

The comparative evaluation is largely treated as a 2-step task. First, the construction of data for evaluation is carried out, and then the optimal AI model for urolithiasis diagnosis is studied by applying technologies such as machine learning, deep learning, and image processing.

In case of applied by machine (deep) learning, regions-of-interest were labeled for ResNet-50 and Fast R-CNN to identify the stone areas in patient data, and the performance of the model was evaluated by comparing the clinical results as ground truth with the model-based guidance. The learning data were classified as normal or abnormal and displayed as sample data to train the model.

In the case of applying the SVM algorithm, an operation of extracting a feature value of an image is performed. Morphological information of stone and intensity information of pixels are used as feature values. The morphological information of stone is pixel connectivity information, considering compactness and elongation [27]. At the same time, the circular object is determined by considering the intensity information of the pixel together and determines the final stone.

Likewise, in the case of watershed, the marker's information also reflects the morphological information of the stone and the intensity information of the pixel. Afterwards, in the extracted area, the final stone is determined in consideration of the compaction and elongation of the area.

And 150 cases of urolithiasis patient data are compared and evaluated through the above various analysis methods. True positive (TP), false negative (FN), and false positive (FP) were calculated by performing 10-fold cross-validation only with the collected still images. Fig. 4 presents definitions of the concepts used in a confusion matrix. Statistical evaluation for assessing categorical and continuous demographic and patient data on SPSS software. Area under the receiver operating characteristic curve (AUC) was used to evaluate the cascading model for pa-

· **TP : The intersection over union (IoU) value is less than 0.3 between the location of a ground-truth stone and the location of a stone detected by the deep learning model on an abnormal image, or an instance where the deep learning model detects a stone in an abnormal image.**

· **FP : The intersection over union (IoU) value is less than 0.3 between the location of a ground-truth stone and the location of a stone detected by the deep learning model on an abnormal image.**

· **FN : The intersection over union (IoU) value is 0.3 or more between the location of a ground-truth stone and the location of a stone detected by the deep learning model on an abnormal image.**

Fig. 4. Definitions of terms used in a confusion matrix.

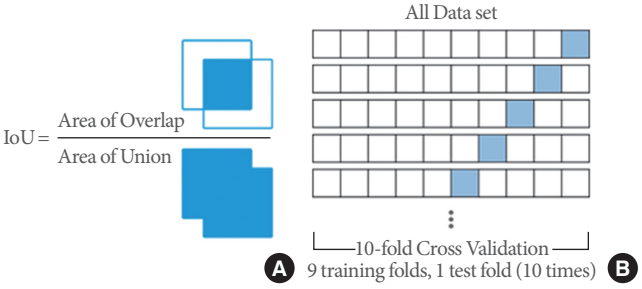

Fig. 5. The intersection over union (IoU) calculation (A) and concept of cross-validation (B).

tient-level prediction for the presence of stones, Sensitivity, specificity, and accuracy were determined for the models from the optimal threshold that was selected on the basis of the sum of sensitivity and specificity on the validation dataset.

RESULTS

The intersection over union calculation and the concept of cross-validation can be explained as shown in Fig. 5, and sensitivity was calculated using the numbers of TP, FP, and FN results. The details are shown in Table 1.

In cross-validation, using a total of 10 sets, 9 learning sets were tested 10 times, and overall, high sensitivity was calculated for 10 sets, thus proving the model's effectiveness. The final value of sensitivity, which is calculated using TP and FN and is a measure of the probability of TP results, showed high recognition accuracy, with an average value of 0.93 for ResNet-50. This finding confirmed that accurate guidance to the stones area was possible when the developed platform was used to support actual surgery. In general, ResNet-50 performed best, but some FP results were derived from normal images. Numerous FP results were detected when the foreign object portion or boundary and grayscale information were very ambiguous. In order to reduce the number of FP results, it seems that further research is needed to improve weight optimization. Since this system is a guide to anatomical structures, FP results may not be of vital real-world importance, but it would be preferable to avoid inaccurate boundary information when supporting surgery in order to minimize unnecessary guidance. Considering these points, it is necessary to various optimization measures that can reduce the number of FP results. Nonetheless, the high sensitivity of the proposed method indicates its accuracy and effectiveness. In addition, AUC is shown in the following Fig. 6 for ResNet-50 only, and good performance can be confirmed.

In the case of Fast R-CNN, similar levels of performance were identified as ResNet-50. However, in some cases of cross-validation, the sensitivity was greatly reduced. It is considered that the features lack updates in response to the object area coordinates. It is believed that this can be advanced through multi-task loss and improvement in the learning structure.

And in the case of SVM, it is thought that there is an issue with the feature value used as the input value. It is mainly processed by using the morphological and intensity information of the stone as feature values, which seems to be an inefficient detection task to perform matching for the entire area. Morphological information considers compactness and elongation, and if the difference between the characteristics of the stone and other object regions is small, it seems that inaccurate results have been derived. To this end, it is considered necessary to use additional characteristic information or to crop and process a separate area of interest.

Table 1. Performance evaluation results of cross-validation

Cross-validation	Sensitivity (TP/FN/FP)			
	ResNet-50	Fast-RCNN	SVM	Watershed
1	0.936 (418/15/150)	0.935 (415/15/153)	0.876 (390/11/178)	0.896 (398/12/170)
2	0.920 (421/22/25)	0.895 (392/20/42)	0.910 (410/22/35)	0.840 (361/22/68)
3	0.927 (426/19/65)	0.906 (410/21/81)	0.798 (371/14/98)	0.924 (424/20/69)
4	0.936 (422/15/210)	0.882 (389/20/232)	0.910 (414/12/218)	0.931 (420/18/212)
5	0.926 (431/20/175)	0.915 (425/18/182)	0.920 (429/29/178)	0.766 (392/12/205)
6	0.941 (428/13/132)	0.944 (430/14/131)	0.864 (398/15/167)	0.841 (391/13/171)
7	0.936 (426/15/167)	0.940 (428/15/162)	0.895 (391/12/193)	0.901 (409/18/178)
8	0.945 (421/11/203)	0.878 (381/15/240)	0.910 (407/14/223)	0.887 (386/11/237)
9	0.943 (415/25/110)	0.910 (399/21/128)	0.812 (372/18/145)	0.882 (389/25/139)
10	0.931 (429/13/149)	0.926 (421/15/151)	0.832 (387/18/179)	0.932 (430/15/145)
Average sensitivity	0.931	0.913	0.873	0.880

TP, true positive; FN, false negative; FP, false positive; SVM, support vector machine.

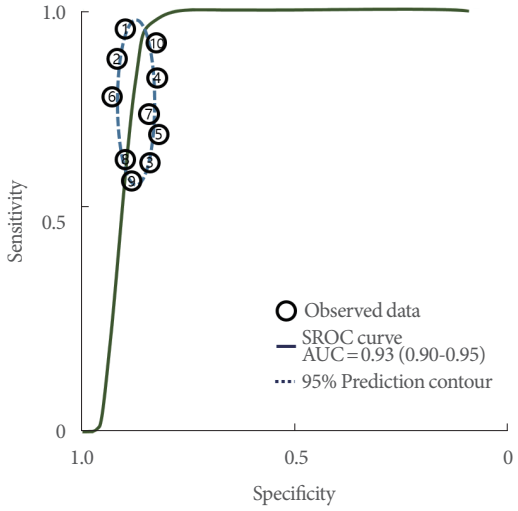

Fig. 6. The area under the receiver operating characteristic curve (AUC) result of ResNet-50. SROC, summary receiver operating characteristic.

Among the image processing methods, the results for watershed that are effective for detecting circular objects showed relatively good performance compared to SVM. This is thought to be possible because marker-based feature information was used instead of a general gradient image. Likewise, the feature information used in the marker is the morphological information and intensity of the stone, and the presence of the final stone is determined through object labeling in the segmented result. Although it is a relatively simple process, it seems that good performance has been detected compared to the SVM algorithm with clear and few considerations.

DISCUSSION

The application of AI has begun in various medical fields. There are no exceptions to the urological system, and AI research is actively being conducted in the cycle before analysis, diagnosis, treatment, and management of urological diseases. Most of them are being studied as an auxiliary means of patient treatment, and the proportion of model research, which is a high core technology.

In this paper, we propose an optimal ureter stone detection model using various AI technologies. The use of AI technology compares and evaluates methods such as machine learning, deep learning, and image processing to find a way to detect ureter stones more effectively. The machine learning method is a SVM method, a representative segmentation method, deep learning is a representative CNN method, ResNet-50 and Fast R-CNN method, and image processing is an efficient watershed for circular objects considering shape information of stones. Comparative evaluation of this method is performed by applying it to abdominal CT images of uremia patients.

Comparative evaluation is largely treated as a 2-step task. First, data construction for evaluation is carried out, and the optimal AI model for urea diagnosis is studied by applying technologies such as machine learning, deep learning, and image processing. In general, ResNet-50 performed best, but some

FP results were derived from generic images. Numerous FP results were detected when the foreign object portion or boundary and grayscale information were very ambiguous. In order to reduce the number of FP results, further research is needed to improve weight optimization. Nevertheless, the high sensitivity of the proposed method exhibits its accuracy and effectiveness. In addition, the AUC is shown in Fig. 6 below for ResNet-50 only, and good performance can be seen.

In the case of Fast R-CNN, it was found to have a similar level of performance to ResNet-50. However, in the case of cross-validation, sensitivity was significantly reduced. It is considered that the function has not been updated in response to the object region coordinates. It is believed that this can be accelerated through multitasking loss and improvement of learning structure.

And there is a problem with the value of a function to be used as input to the case of SVM. Mainly stone in the form of strength as the value information and data processing for the entire area, which is matched too inefficient to carry out detection work seems to be. morphological characteristics of the area, stones and other objects to take into account the information density and height difference seems to be inaccurate results if you are. To that end, additional attribute information need to be processed into separate areas of interest.

Among the image processing methods, the results for watershed, which is effective for detecting circular objects, showed relatively superior performance compared to SVM. This is thought to be possible because marker-based feature information was used instead of a general gradient image. Although it is a relatively simple process, good performance seems to be detected compared to SVM algorithms with clear and few considerations.

As a result, the general situation in the most effective way to the detection stone can be found. But a variety of variables may slightly different is the difference through the term could tell. As a future works, urological diseases are diverse and the research will be expanded by customizing AI models specialized for those diseases.

AUTHOR CONTRIBUTION STATEMENT

Conceptualization: *KHK*
Data curation: *MSY*
Formal analysis: *SJE*
Funding acquisition: *KHK*
Methodology: *SJE*
Project administration: *TKW*
Visualization: *SJE*
Writing - original draft: *SJE*
Writing - review & editing: *KHK*

ORCID

Sung-Jong Eun	0000-0003-3063-0452
Myoung Suk Yun	0000-0001-6602-2630
Taeg-Keun Whangbo	0000-0003-1409-0580
Khae-Hawn Kim	0000-0002-7045-8004

REFERENCES

1. Konstantinos-Vaios M, Athanasios O, Ioannis S, Marina K, George M, Evangelia N, et al. Defining voiding dysfunction in women: bladder outflow obstruction versus detrusor underactivity. Int Neurourol J 2021;25:244-51.
2. Yu J, Jeong BC, Jeon SS, Lee SW, Lee KS. Comparison of efficacy of different surgical techniques for benign prostatic obstruction. Int Neurourol J 2021;25:252-62.
3. Mytilekas KV, Oeconomou A, Sokolakis I, Kalaitzi M, Mouzakitis G, Nakopoulou E, et al. Defining voiding dysfunction in women: bladder outflow obstruction versus detrusor underactivity. Int Neurourol J 2021;25:244-51.
4. Kim HW, Lee JZ, Shin DG. Pathophysiology and management of long-term complications after transvaginal urethral diverticulectomy. Int Neurourol J 2021;25:202-9.
5. Jang EB, Hong SH, Kim KS, Park SY, Kim YT, Yoon YE, et al. Catheter-related bladder discomfort: how can we manage it? Int Neurourol J 2020;24:324-31.
6. Kwon WA, Lee SY, Jeong TY, Moon HS. Lower urinary tract symptoms in prostate cancer patients treated with radiation therapy: past and present. Int Neurourol J 2021;25:119-27.
7. Baser A, Zumrutbas AE, Ozlulerden Y, Alkıs O, Oztekın A, Celen S, et al. Is there a correlation between behçet disease and lower urinary tract symptoms? Int Neurourol J 2020;24:150-5.
8. Kim SJ, Choo HJ, Yoon H. Diagnostic value of the maximum urethral closing pressure in women with overactive bladder symptoms and functional bladder outlet obstruction. Int Neurourol J 2022;26(Suppl 1):S1-7.
9. Wen L, Li X, Gao L. A transfer convolutional neural network for fault diagnosis based on ResNet-50. Neural Comput Appl 2020;32:6111-24.

10. Kim JW, Kim SJ, Park JM, Na YG, Kim KH. Past, present, and future in the study of neural control of the lower urinary tract. Int Neurourol J 2020;24:191-9.
11. Koonce B. Convolutional neural networks with swift for tensorflow. Berkeley (CA): Apress; 2021. p. 63-72.
12. Quach LD, Quoc NP, Thi NH, Tran DC, Hassan MF. Using surf to improve resnet-50 model for poultry disease recognition algorithm. In: 2020 International Conference on Computational Intelligence (ICCI); 2020 Oct 8-9; Bandar Seri Iskandar, Malaysia. Manhattan (NY): IEEE; 2020. p. 317-21.
13. Miranda ND, Novamizanti L, Rizal S. Convolutional Neural Network pada klasifikasi sidik jari menggunakan RESNET-50. J Tek Inf 2020;1:61-8.
14. Esteva A, Kuprel B, Novoa RA, Ko J, Swetter SM, Blau HM, et al. Dermatologist-level classification of skin cancer with deep neural networks. Nature 2017;542:115-8.
15. Lecun Y, Bottou L, Bengio Y, Haffner P. Gradient-based learning applied to document recognition. Proc IEEE 1998;86:2278-324.
16. ImageNet [Internet]. c2022 [cited 2022 Jan 20]. Available from: http://image-net.org/.
17. Flickr [Internet]. c2022 [cited 2022 Jan 15]. Available from: https://www.flickr.com/.
18. INRIA Person dataset [Internet]. c2022 [cited 2022 Jan 12]. Available from: http://pascal.inrialpes.fr/data/human/.
19. Zeiler MD, Fergus R. Visualizing and understanding convolutional networks. European conference on computer vision. arXiv:1311.2901. https://doi.org/10.48550/arXiv.1311.2901
20. Krizhevsky A, Sutskever I, Hinton GE. ImageNet classification with deep convolutional neural networks. NIPS'12: Proceedings of the 25th International Conference on Neural Information Processing Systems; 2012 Dec 3-6; Lake Tahoe Nevada. Red Hook (NY): Curran Associates Inc.; 2012. p. 1097-105.
21. Szegedy C, Liu W, Jia Y, Sermanet P, Reed S, Anguelov D, et al. Going deeper with convolutions. In: 2015 IEEE Conference on Computer Vision and Pattern Recognition (CVPR); 2015 Oct 15; Boston, USA. IEEE 2015;1-9.
22. Kim MK. Feature extraction on a periocular region and person authentication using a ResNet Model. J Korea Multimed Soc 2019;22:1347-55.
23. Uijlings JRR, van de Sande KEA, Gevers T, Smeulders AWM. Selective search for object recognition. Int J Comput Vis 2013;104:154-71.
24. Girshick R. Fast R-CNN In: 2015 IEEE International Conference on Computer Vision (ICCV); 2015 Dec 7-13; Santiago, Chile. IEEE 2015. p. 1440-8.
25. Vapnik V, Mukherjee S. Support vector method for multivariate density estimation. Adv Neural Inf Process Syst 2000;659-65.
26. Najman L, Schmitt M. Watershed of a continuous function. Sig Process (Spec Issue Math Morphol) 1994;38:99-112.
27. Eun SJ, Whangbo TK. Efficient circular-shape object segmentation method for adjacent objects. Multimed Tools Appl 2015;74:8951-59.